

Entropy dependence of correlations in one-dimensional $SU(N)$ antiferromagnets

Laura Messio¹ and Frédéric Mila²

¹*Institut de Physique Théorique (IPhT), CEA, CNRS, URA 2306, F-91191 Gif-sur-Yvette, France*

²*Institute of Theoretical Physics, École Polytechnique Fédérale de Lausanne (EPFL), CH-1015 Lausanne, Switzerland*

(Dated: November 27, 2024)

Motivated by the possibility to load multi-color fermionic atoms in optical lattices, we study the entropy dependence of the properties of the one-dimensional antiferromagnetic $SU(N)$ Heisenberg model, the effective model of the $SU(N)$ Hubbard model with one particle per site (filling $1/N$). Using continuous-time world line Monte Carlo simulations for $N = 2$ to 5, we show that characteristic short-range correlations develop at low temperature as a precursor of the ground state algebraic correlations. We also calculate the entropy as a function of temperature, and we show that the first sign of short-range order appears at an entropy per particle that increases with N and already reaches $0.8k_B$ at $N = 4$, in the range of experimentally accessible values.

PACS numbers: 67.85.-d, 75.10.Jm, 02.70.-c

Lattice $SU(N)$ models play an ever increasing role in the investigation of strongly correlated systems, both in condensed matter and in cold atoms. The first systematic use of these models took place in the context of the large- N generalization of the $SU(2)$ Heisenberg model, in which conjugate (or self-conjugate) representations are put on the two sublattices of the square lattice so that a $SU(N)$ singlet can be formed on two sites¹⁻³. Over the years, another class of $SU(N)$ models with the same representation at each site has appeared as the relevant description of the low temperature properties in several contexts. In particular, the $SU(3)$ model corresponds to the spin-1 Heisenberg model with equal bilinear and biquadratic interactions⁴⁻⁶, while the $SU(4)$ model is equivalent to the symmetric version of the Kugel-Khomskii model of Mott insulators with orbital degeneracy^{7,8}. These models have however attracted renewed attention recently as the appropriate low energy theory of ultracold gases of alkaline-earth-metal atoms in optical lattices in the Mott insulating phase with one atom per site, the parameter N corresponding to the number of internal degrees of freedom of the atoms⁹.

A peculiar characteristic of these $SU(N)$ models is that one needs N sites to form a singlet. This is often reflected in their ground state properties. In one dimension, the $SU(N)$ model has been solved with Bethe ansatz for arbitrary N ¹⁰, and the dispersion of the elementary fractional excitations has a periodicity $2\pi/N$. On a ladder, the $SU(4)$ model has a plaquette ground state¹¹. In two-dimensions, the $SU(3)$ model on both the square and triangular lattices has long-range color order with 3-site periodicity along the lines^{4,5}, while on the kagome lattice it is spontaneously trimerized¹². The $SU(4)$ model on the checkerboard lattice also has a plaquette ground state¹². Even on the square lattice, where the $SU(4)$ model undergoes spontaneous dimerization¹³ with possibly algebraic correlations¹⁴, neighboring dimers involved pairs of different colors, so that the 4 colors are indeed present with equal weight on all plaquettes. The general properties for arbitrary N are not known however. An adaptation of the previous large- N studies has been proposed for m atoms per site¹⁵. If $m = O(N)$, the ground state has been proposed to be a chiral spin liquid for large N .

The wealth of ground states predicted for different N on

various lattices calls for an experimental investigation. Ultracold fermionic atoms can a priori lead to very accurate realizations of these models. However, the temperature is a limiting factor. It can be lowered with respect to the initial temperature if the optical lattice is adiabatically switched on¹⁶, but it cannot be made arbitrarily small. In fact, with adiabatic switching, one can control the entropy rather than the temperature, and in current state-of-the-art experimental setups, the lower limit for fermions with $N = 2$ is equal to $0.77k_B$ per particle¹⁷. If contact is to be made with experiments on cold atoms, it is thus crucial to know the properties of a given model as a function of entropy. For the $SU(2)$ Heisenberg model on the cubic lattice, Néel ordering takes place at an entropy $0.338 k_B$, i.e. about half the value that can be achieved today¹⁷.

The first hint that increasing the number of colors might help in beating this experimental limit has been obtained in the context of a high temperature investigation of the N -flavour Hubbard model by Hazzard et al¹⁸, who have shown that the effective temperature reached after introducing the optical lattice decreases with N under fairly general conditions. However, to the best of our knowledge, no attempt has been made so far to determine how the temperature or the entropy below which signatures of the ordering will show up depends on N .

In this Letter, we address this issue in the context of the one-dimensional (1D) antiferromagnetic $SU(N)$ Heisenberg model on the basis of extensive Quantum Monte Carlo (QMC) simulations. As we shall see, the ground state algebraic correlations lead to characteristic anomalies in the structure factor upon lowering the temperature. These anomalies only become visible at quite low temperature, but remarkably enough, the corresponding entropy per particle increases with N , leading to observable qualitative effects with current experimental setups for $N \geq 4$.

The $SU(N)$ Heisenberg model.— A good starting point to discuss N -color fermionic atoms loaded in an optical lattice is the $SU(N)$ Hubbard model defined by the Hamiltonian:

$$\hat{H} = t \sum_{\langle i,j \rangle \alpha} (\hat{c}_{\alpha i}^\dagger \hat{c}_{\alpha j} + h.c.) + U \sum_{i, \alpha < \beta} \hat{n}_{\alpha i} \hat{n}_{\beta i}, \quad (1)$$

where $\hat{c}_{i,\alpha}^\dagger$ and $\hat{c}_{i,\alpha}$ are creation and annihilation operators of

a fermion of color $\alpha = 1 \dots N$ on site i and the sum is over the first-neighbors of a periodic chain of length L . $\hat{n}_{\alpha i}$ is the number of fermions of color α on site i . At filling $1/N$, i.e. with one fermion per site, the ground state is a Mott insulator, and to second order in t/U , the low-energy effective Hamiltonian is the $SU(N)$ Heisenberg model with the fundamental $SU(N)$ representation at each site, and with coupling constant $J = 2t^2/U$. Setting the energy unit by $J = 1$, this Hamiltonian can be written (up to an additive constant):

$$\hat{H} = \sum_{\langle ij \rangle} \hat{P}_{ij}. \quad (2)$$

where \hat{P}_{ij} permutes the colors on sites i and j . If we denote by $\hat{S}_i^{\alpha\beta}$ the operator that replaces color β by α on site i , this permutation operator can be written as:

$$\hat{P}_{ij} = \sum_{\alpha, \beta} \hat{S}_i^{\alpha\beta} \hat{S}_j^{\beta\alpha} \quad (3)$$

This effective Hamiltonian is an accurate description of the system provided the temperature is much smaller than the Mott gap. In terms of entropy, the criterion is actually quite simple. The high temperature limit of the entropy per site of the $SU(N)$ Hubbard model at $1/N$ -filling can be shown to be equal to $k_B(N \ln N - (N-1) \ln(N-1))$, while that of the $SU(N)$ Heisenberg model is equal to $k_B \ln N$. So we expect the description in terms of the Heisenberg model to be accurate when the entropy is below $k_B \ln N$. For $SU(2)$, this is a severe restriction for experiments since $\ln 2 \simeq 0.693\dots$, but already for $SU(3)$, this is less of a problem since $\ln 3 \simeq 1.099$. Of course, this is not the whole story since what really matters is the entropy below which specific correlations develop, but this is an additional motivation to consider $SU(N)$ models with $N > 2$.

Exact results.— A number of exact results that have been obtained over the years on the 1D $SU(N)$ Heisenberg model will prove to be useful. The model has been solved with Bethe ansatz by Sutherland¹⁰. He showed that, in the thermodynamic limit, the energy per site is given by

$$E_0(N) = 2 \sum_{k=2}^{\infty} \frac{(-1)^k \zeta(k)}{N^k} - 1, \quad (4)$$

where ζ is the Riemann's zeta function. Some values are given in Tab. II. In addition, he showed that there are $N-1$ branches of elementary excitations which all have the same velocity $v = 2\pi/N$ at small k . Affleck has argued that the central charge c should be equal to $N-1$ ¹⁹, and Lee has shown that²⁰, at low temperature T , the entropy is given by:

$$S(T) = \frac{k_B N(N-1)}{6} T + O(T^2), \quad (5)$$

a direct consequence of $c = N-1$ and $v = 2\pi/N$ since the linear coefficient is equal to $\pi c/3v$.

The QMC algorithm.— Quantum Monte-Carlo is the most efficient method to study the finite temperature properties of interacting systems provided one can find a basis where there

is no minus sign problem, i.e. a basis in which all off-diagonal matrix elements of the Hamiltonian are non-positive. For the $SU(2)$ antiferromagnetic Heisenberg model on bipartite lattices, this is easily achieved by a spin-rotation by π on one sublattice. For $SU(N)$ with $N > 2$, there is no such general solution, but in 1D one can get rid of the minus sign on a chain with open boundary conditions, as already noticed for the $SU(4)$ model²¹. Let us start from the natural basis consisting of the N^L product states $\otimes_i |\alpha_i\rangle = |\alpha_0, \dots, \alpha_{L-1}\rangle$, where α_i is the color at site i . In this basis, all off-diagonal elements of the $SU(N)$ model of Eq. 2 are either zero or positive. However, a generalization of the Jordan-Wigner transformation allows to change all these signs on an open chain. This transformation is defined by:

$$|\alpha_0, \dots, \alpha_{L-1}\rangle \rightarrow (-1)^{r(\alpha_0, \dots, \alpha_{L-1})} |\alpha_0, \dots, \alpha_{L-1}\rangle, \quad (6)$$

where $r(\alpha_0, \dots, \alpha_{L-1})$ is the number of permutations between different color particles on neighboring sites needed to obtain a state such that the α_i are ordered ($\alpha_i \leq \alpha_j$ for $i < j$). This basis change is equivalent to a Hamiltonian transformation, the new Hamiltonian being given by:

$$\hat{H} = \sum_{\langle ij \rangle} \sum_{\alpha} \left(\hat{S}_i^{\alpha\alpha} \hat{S}_j^{\alpha\alpha} - \sum_{\beta \neq \alpha} \hat{S}_i^{\alpha\beta} \hat{S}_j^{\beta\alpha} \right). \quad (7)$$

On a periodic chain, the equivalence with the Hamiltonian of Eq. 2 is not exact, but the difference disappears in the thermodynamic limit. So in the following we will simulate the Hamiltonian of Eq. 7.

To do so, we have developed a continuous time world-line algorithm with cluster updates²² adapted to the model of Eq. 7 with N colors. The partition function Z is expressed as a path integral over the configurations $\phi : \tau \rightarrow \phi(\tau)$, where τ is the imaginary time going from 0 to $\beta = \frac{1}{k_B T}$ and $\phi(\tau)$ is a basis state. The functions ϕ that contribute to the integral can be represented by $\phi(0)$ and by a set of world line crossings $\{(i, j, \tau)\}$ that exchange the colors of two sites i and j at time τ . A local configuration c on a link ij at time τ is represented by

$$c = \begin{pmatrix} \alpha_i(\tau^+) \alpha_j(\tau^+) \\ \alpha_i(\tau^-) \alpha_j(\tau^-) \end{pmatrix} \quad (8)$$

Cluster algorithms are well documented for 2-color models. Here we generalize the approach to $SU(N)$ by choosing randomly two different colors p and q out of N and by constructing clusters on which only these two colors are encountered. The steps to construct the clusters are the following. We first randomly place elementary graphs in the configuration using a Poisson distribution. These graphs are drawn in the first column of Tab. I and the Poisson time constant is given in the last column. They are accepted only if $\Delta_G(c) = 1$ (if a color which is neither p nor q appears in the local configuration, the graph is rejected). Then we assign graphs to the world-line crossings between p and q colors using the last two columns of Tab. I. At the places where no graph has been attributed, we follow the path with the same color. Finally we follow

G	$\Delta_G \begin{pmatrix} pp \\ pp \end{pmatrix}$	$\Delta_G \begin{pmatrix} pq \\ pq \end{pmatrix}$	$\Delta_G \begin{pmatrix} qp \\ qp \end{pmatrix}$	W_G
	1	—	1	ϵ
	—	1	1	$1 - \epsilon$
	0	1	0	2ϵ

TABLE I: Fabrication rules for clusters. In the first column are drawn all possible graphs G . The three following columns are $\Delta_G(c)$ equal to 1 when G is compatible with the local configuration c . The last column is the constant of time used to sample the graphs with a Poisson law. ϵ is a small number ensuring the ergodicity (ϵ is taken 0.01 in our simulations).

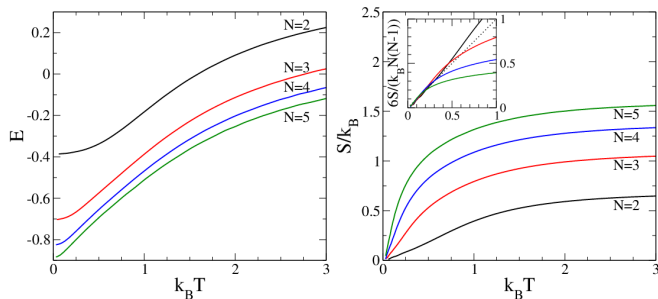


FIG. 1: Evolution of the energy per site E and of the entropy per site S as a function of the temperature T for different N on a $L = 60$ chain. The inset shows the slope of the entropy at $T = 0$, given in Eq. 5. The curvature being positive at $T = 0$, the curves go higher than the tangent (dashed line).

each constructed cluster and exchange p and q on it with a probability $1/2$ (Swendsen-Wang algorithm). This constitutes a Monte Carlo step.

Using this algorithm, we have calculated the energy per site E , which is given by:

$$E = \left\langle \frac{\hat{H}}{L} \right\rangle \simeq \frac{k_B T}{L n} \sum_{\phi} \left(\sum_{\langle ij \rangle} \int d\tau \delta_{\alpha_i(\tau), \alpha_j(\tau)} - n(\phi) \right), \quad (9)$$

where n is the number of Monte Carlo steps and $n(\phi)$ the number of world-line crossings in the configuration ϕ , the diagonal correlations defined by

$$C(j) = \left\langle \sum_{\alpha} \hat{S}_0^{\alpha\alpha} \hat{S}_j^{\alpha\alpha} \right\rangle - \frac{1}{N} \quad (10)$$

and the associated structure factor defined by

$$\tilde{C}(k) = \frac{1}{2\pi} \frac{N}{N-1} \sum_j C(j) e^{ikj}. \quad (11)$$

This structure factor is normalized in such a way that $\frac{2\pi}{L} \sum_k \tilde{C}(k) = 1$.

The results.— We have studied chains of length $L = 60$ for T from 0.01 to 20 with a number of colors $N = 2, 3, 4$

N	$BA(L = \infty)$	$BA(L = 60)$	$QMC(L = 60)$
2	-0.386294		-0.38675(2)
3	-0.703212	-0.7038228	-0.70384(2)
4	-0.8251193		-0.82577(2)
5	-0.884730		-0.88541(2)

TABLE II: Ground state energies per site obtained for several N with the Bethe Ansatz (BA) in the thermodynamic limit and on a finite size chain²³, and at $T = 0.01$ with the quantum Monte-Carlo algorithm (see text) on a $L = 60$ chain and $n = 10^7$ Monte-Carlo steps.

and 5, and a number of Monte Carlo steps n at least equal to 10^6 . The correlation time measured by the binning method indicates that around N steps are needed to obtain uncorrelated configurations, whatever the temperature, and that the precision on the energy per site E is better than 10^{-4} . This could be confirmed by the comparison of the limit of the energy when $T \rightarrow 0$ with the exact finite L value for $SU(3)$.²³ Moreover, the energy of the ground state differs from that of the thermodynamic limit by less than 8.10^{-4} . So, for our purpose, the finite size effects can be considered to be negligible (see Tab. II). The entropy per site S has been deduced from the energy E by an integration from high temperature:

$$S(T) = S(\infty) - \int_T^{\infty} d\tau \frac{k_B}{\tau} \frac{dE}{d\tau} \quad (12)$$

where $S(\infty) = k_B \ln(N)$. E and S are plotted in Fig. 1 for different N as a function of T . Since the entropy is the result of a numerical integration, it is important to check its accuracy, especially at low temperature since by construction it has to be correct at high temperature. Now, we know that, at low temperature, the entropy must be linear with a slope equal to $k_B N(N-1)/6$ (see Eq.5). This is confirmed by the inset of Fig. 1b), in which one clearly sees that the entropies times $6/k_B N(N-1)$ lie on top of each other at low temperature.

Now, the stabilization of the energy at low T occurs at a temperature that decreases when N increases. Thus, one could naively think that it will be more difficult to observe the development of the ground state correlations when N increases. However, this is not true if one considers the entropy. Indeed, the entropy grows much faster at low temperature when increasing N . So, the temperature corresponding to a given entropy decreases very fast when N increases.

We now look at the diagonal correlations $\tilde{C}(k)$. They have been calculated for different temperatures, but, in view of the implications for ultracold fermionic gas, we represent them as a function of the entropy per site S . Since the system is 1D, there is no long range order, hence no Bragg peaks. Nevertheless, short-range correlation develop at low entropy. They translate into finite height peaks in $\tilde{C}(k)$ at finite temperature, and singularities at zero temperature. The number and the position of these peaks depend on the number of colors N . From the Bethe ansatz solution, singularities are expected to occur at $k = 2p\pi/N$ with $p = 1, \dots, N-1$. The results of Fig. 2 agree with this prediction: there is a single peak at π for

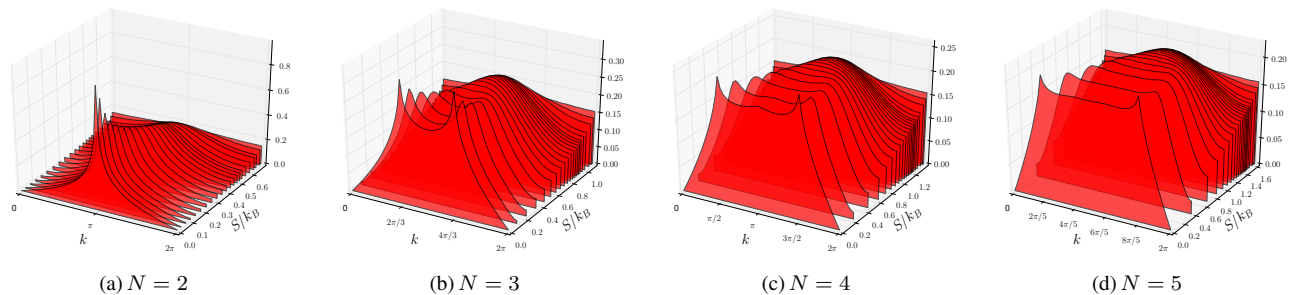


FIG. 2: Evolution of the structure factor $\tilde{C}(k)$ as a function of the entropy per site S for different N on a $L = 60$ chain.

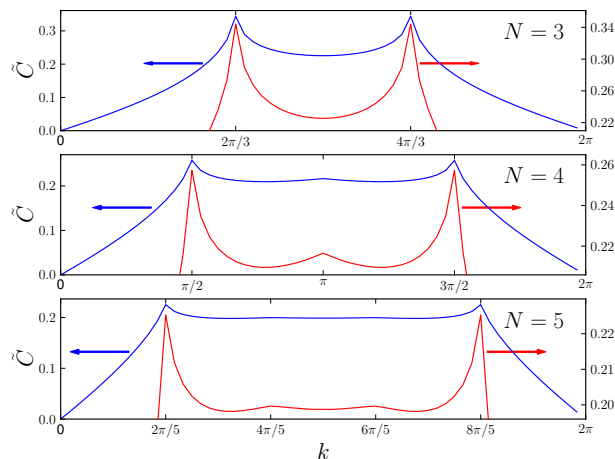


FIG. 3: Structures factor $\tilde{C}(k)$ at low temperature ($k_B T = 0.01$) for different N on a $L = 60$ chain, with $n = 10^7$ Monte-Carlo steps. Small peaks are clearly visible at $k = \pi$ for $N = 4$ and $k = 4\pi/5$ and $6\pi/5$ for $N = 5$. The data for $N = 4$ are in perfect agreement with those of Ref.21.

$SU(2)$, while $N - 1$ peaks are indeed present for $SU(N)$ at sufficiently small entropy. Note however that all peaks do not have the same amplitude for $N \geq 4$. For $N = 4$ and 5 , two types of peaks not related by the symmetry $k \rightarrow 2\pi - k$ are present. The peaks at $2\pi/N$ and $2(N-1)\pi/N$ are much more prominent, and they start to be visible at much larger entropy.

At the maximal entropy, the structure factor $\tilde{C}(k)$ is flat (see Fig. 2). At large but finite entropy, it presents a broad maximum at $k = \pi$ for all N . This reflects the simple fact that colors tend to be different on neighboring sites. More specific correlations appear upon lowering the entropy. For $SU(2)$, the peak at $k = \pi$ just gets more pronounced. To observe the development of the singularity typical of the $SU(2)$ ground state algebraic correlations will however require to reach rather low entropy. This should be contrasted with the $N > 2$ cases, where a qualitative change in the structure factor occurs upon

reducing the entropy: the broad peak at $k = \pi$ is replaced by peaks at $2\pi/N$ and $2(N-1)\pi/N$. One can in principle read off the corresponding entropy from Fig. 2. To come up with a quantitative estimate, we note that, upon reducing the entropy, the curvature of the structure factor at $k = \pi$ changes sign from positive at high temperature to negative when the peaks at $2\pi/N$ and $2(N-1)\pi/N$ appear. This occurs at $S_c/k_B = 0.58, 0.87$ and 1.08 for $N = 3, 4$ and 5 respectively. This characteristic entropy S_c increases more or less linearly with N as $S_c \simeq 0.2Nk_B$, and for $N = 4$ and 5 , it lies in the experimentally accessible range. This is mostly a consequence of the temperature dependence of the entropy, which grows much faster with N at low temperature. The characteristic temperature at which deviations from the broad peak at $k = \pi$ occur depends only weakly on N . Finally, secondary peaks appear at lower temperature (see Fig. 3)

Conclusions.— We have shown that the entropy at which the periodicity characteristic of the zero temperature algebraic order of $SU(N)$ chains is revealed increases significantly with N . For $N = 4$, this entropy is already larger than the entropy per particle recently achieved in the $N = 2$ case in the center of the Mott insulating cloud ($0.77 k_B$)¹⁷. Whether a similar entropy can be achieved for $N > 3$ remains to be seen. As shown by Hazzard et al¹⁸, if the initial temperature is fixed, the initial entropy in a 3D trap increases with N as $N^{1/3}$, implying that one might have to go to values of N larger than 4 to reach a final entropy low enough to observe characteristic correlations. However, evaporative cooling might allow to reach initial entropies that are less dependent on N . In a recent experiment on ¹⁷³Yb, the initial entropy reported by Sugawa et al²⁴ for this $N = 6$ case is not much higher than in $N = 2$ experiments¹⁷. It is our hope that the present results will encourage the experimental investigation of the $1/N$ -filled Mott phase of N -color ultracold fermionic atoms.

We thank Daniel Greif for useful discussions. LM acknowledges the hospitality of EPFL, where most of this project has been performed. This work has been supported by the Swiss National Fund and by MaNEP.

¹ I. Affleck and J. B. Marston, *Phys. Rev. B* **37**, 3774 (1988).

² N. Read and S. Sachdev, *Nuclear Physics B* **316**, 609 (1989).

- ³ D. P. Arovas and A. Auerbach, *Phys. Rev. B* **38**, 316 (1988).
- ⁴ A. Läuchli, F. Mila, and K. Penc, *Phys. Rev. Lett.* **97**, 087205 (2006).
- ⁵ T. A. Tóth, A. M. Läuchli, F. Mila, and K. Penc, *Phys. Rev. Lett.* **105**, 265301 (2010).
- ⁶ B. Bauer, P. Corboz, A. M. Läuchli, L. Messio, K. Penc, M. Troyer, and F. Mila, *Phys. Rev. B* **85**, 125116 (2012).
- ⁷ K. I. Kugel' and D. I. Khomskii, *Soviet Physics Uspekhi* **25**, 231 (1982).
- ⁸ Y. Q. Li, M. Ma, D. N. Shi, and F. C. Zhang, *Phys. Rev. Lett.* **81**, 3527 (1998).
- ⁹ A. V. Gorshkov, M. Hermele, V. Gurarie, C. Xu, P. S. Julienne, J. Ye, P. Zoller, E. Demler, M. D. Lukin, and A. M. Rey, *Nature Physics* **6**, 289 (2010).
- ¹⁰ B. Sutherland, *Phys. Rev. B* **12**, 3795 (1975).
- ¹¹ M. van den Bossche, P. Azaria, P. Lecheminant, and F. Mila, *Phys. Rev. Lett.* **86**, 4124 (2001).
- ¹² P. Corboz, K. Penc, F. Mila, and A. M. Laeuchli, *ArXiv e-prints* (2012), [arXiv:1204.6682 \[cond-mat.str-el\]](https://arxiv.org/abs/1204.6682) .
- ¹³ P. Corboz, A. M. Läuchli, K. Penc, M. Troyer, and F. Mila, *Phys. Rev. Lett.* **107**, 215301 (2011).
- ¹⁴ F. Wang and A. Vishwanath, *Phys. Rev. B* **80**, 064413 (2009).
- ¹⁵ M. Hermele, V. Gurarie, and A. M. Rey, *Phys. Rev. Lett.* **103**, 135301 (2009).
- ¹⁶ F. Werner, O. Parcollet, A. Georges, and S. R. Hassan, *Phys. Rev. Lett.* **95**, 056401 (2005).
- ¹⁷ R. Jördens, L. Tarruell, D. Greif, T. Uehlinger, N. Strohmaier, H. Moritz, T. Esslinger, L. De Leo, C. Kollath, A. Georges, V. Scarola, L. Pollet, E. Burovski, E. Kozik, and M. Troyer, *Phys. Rev. Lett.* **104**, 180401 (2010).
- ¹⁸ K. R. A. Hazzard, V. Gurarie, M. Hermele, and A. M. Rey, *Phys. Rev. A* **85**, 041604 (2012).
- ¹⁹ I. Affleck, *Nuclear Physics B* **305**, 582 (1988).
- ²⁰ K. Lee, *Physics Letters A* **187**, 112 (1994).
- ²¹ B. Frischmuth, F. Mila, and M. Troyer, *Phys. Rev. Lett.* **82**, 835 (1999).
- ²² N. Kawashima and K. Harada, *Journal of the Physical Society of Japan* **73**, 1379 (2004).
- ²³ F. C. Alcaraz and M. J. Martins, *Journal of Physics A: Mathematical and General* **22**, L865 (1989).
- ²⁴ S. Sugawa, K. Inaba, S. Taie, R. Yamazaki, M. Yamashita, and Y. Takahashi, *Nat Phys* **7**, 642 (2011).